International Journal of Computer and Communication Technology

Volume 1 | Issue 3 Article 2

July 2010

Design and Simulation of Rotary Field Ferrite Phase Shifter using Ansoft HFSS

Parul Dawar
Department Of Electronics and Communications, Guru Tegh Bahadur Institute of Technology, Rajouri Garden,new Delhi-110064, paru.dawar@gmail.com

Recommended Citation
Dawar, Parul (2010) "Design and Simulation of Rotary Field Ferrite Phase Shifter using Ansoft HFSS," *International Journal of Computer and Communication Technology*: Vol. 1 : Iss. 3 , Article 2.
DOI: 10.47893/IJCCT.2010.1038
Available at: https://www.interscience.in/ijcct/vol1/iss3/2

Design and Simulation of Rotary Field Ferrite Phase Shifter using Ansoft HFSS

Parul Dawar

Department Of Electronics and Communications, Guru Tegh Bahadur Institute of Technology,

Rajouri Garden,new Delhi-110064

paru.dawar@gmail.com [1]

***Abstract*—HFSS is a high-performance full-wave electromagnetic (EM) field simulator for arbitrary 3D volumetric passive device modeling.It employs the Finite Element Method (FEM), adaptive meshing, and brilliant graphics. This paper reports the measured phase shift characteristics of C-band phase shifters constructed from lithium ferrites. This is done by first magnetizing the ferrite rod in perpendicular (to direction of propagation) direction and then in longitudinal (parallel to direction of propagation). Thereby, giving a phase shift of 90 degrees. It has been proved that by giving a phase shift of 90 degrees to the magnetic field, we will get the phase shift of twice the rotation i.e. 180 degrees.**

Keywords*— *Microwave, HFSS, Ferrite phase shifters, Ferrite waveguides, Magnetic microwave devices

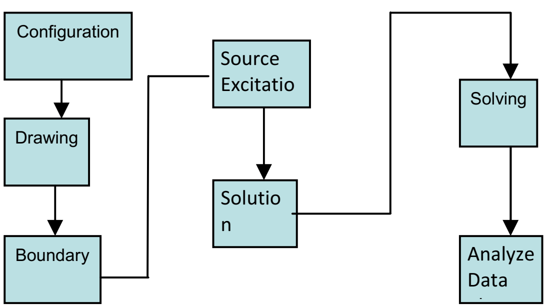

Fig 1: Procedure to simulate objects in HFSS.

I. DESIGNING

A. Construction

The basic functional diagram of the rotary field phase shifter is sketched in Fig 2

.

Fig 2: Functional block diagram of ferrite rotary-field phase shifter

A central field rotatable half wave plate is coupled at each end to fixed quarter wave plates that in turn couple to transducers to waveguide or other transmission structure.

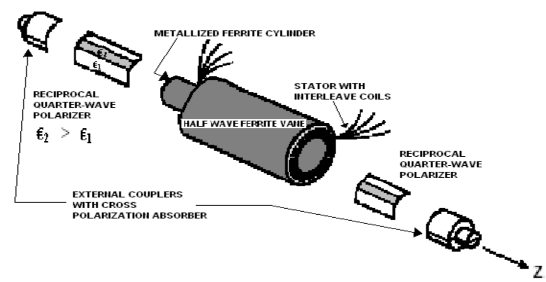

Fig 3: Sketch of internal parts of a typical ferrite rotary-field phase shifter, showing drive stator with ferrite rod, dielectric quarter wave plates, and transducers prior to metallization

Fig 3 sketches a practical realization consisting of a central ferrite cylinder which completely fills a circular waveguide and which is coupled at each end to ceramic dielectric assemblies that in homogeneously fill the waveguide. These dielectric quarter wave plate sections convert linear polarization incident at either end in to circularly polarized TE_{11} mode waves at the interface with the ferrite section. Beyond the dielectric quarter–wave plates are transducers coupling the circular waveguide to ordinary rectangular guide, and at the same time absorbing any energy cross–polarized to the propagating wave orientation. The ferrite is biased with a transverse four pole magnetic field to a level that creates a birefringence of 180° differential phase (i.e. a half–wave plate).

B. Principle of operation

It is a magnetically variable version of the rotary vane phase shifter. Resistive films are incorporated in the matching section to absorb any unwanted cross-polarized modes. Outside the metallic waveguide wall, a ferrite frame known as multi-pole yoke is placed which physically resembles a motor stator, containing sine and cosine orthogonal windings. These windings produce a transverse four-pole magnetic field. This transverse field with quadrupole characteristics has a much stronger interaction with the ferrite than that of bipolar field case. The ferrite rod is biased with this transverse four-pole magnetic field to a level that creates a birefringence of 180^o differential phase (i.e. half wave plate).

C. Sample preparation

The properties of ferrite rod material are in table 1 below.

TABLE 1: ROD MATERIAL CHARACTERISTICS

Material	Li-Ti ferrite
Saturation Magnetization $4\pi Ms$	1250 Gauss
Remanence R	0.9
Curie temperature, Tc	≈ 310oC
Dielectric constant €'	17.5
Resonance linewidth ΔH	≈300 Oe
Dielectric loss tangent tanδ	<=0.0005

There lies a strong possibility of coupling occurring between the dominant TE_{11} mode and any mode with quadrantal symmetry because of distortion produced by the transverse bias field in rod medium. Therefore, the rod diameter is chosen such that the highest operating frequency is below the cut-off frequency of TE_{21} mode. The cut-off frequency of TE_{21} mode is taken as 5.9 GHz which is the highest operating frequency. For TE_{21} mode cut-off

$$fc = 3.054/\pi d(\mu€)^{1/2} \quad (1)$$

The diameter is chosen as 12.2 mm which is lower than the maximum diameter obtained to keep a safe margin for onset of higher order modes. The ferrite rod is to be metallized using electroplating, so that it acts as a circular waveguide. The skin depth of silver at 5.7 GHz is computed to be 0.85μm. Hence the coating thickness of order of 3μm which lies between 3-4 times of skin depth.

D. Design on HFSS

D.1 The ferrite rod specifying cut-off frequency as 5.9 GHz ,as in Fig 4(a), was designed and waveports assigned on either ends of rod as in fig 4(b) and fig 4(c)

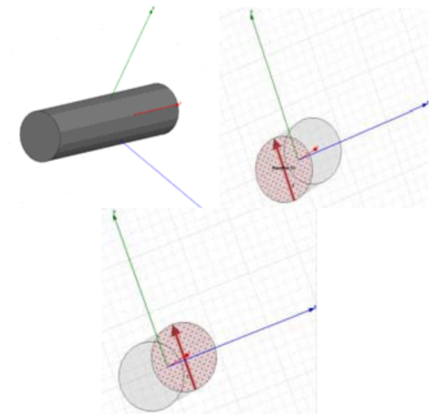

Fig 4(a) Fig 4(b) Fig 4(c)

D.2. Analysis result for sweep frequency from 5.4 GHz to 5.9 GHz of S_{11} and S_{22} is in Fig 4(d)and S_{12} and S_{21} is in Fig 4(e)

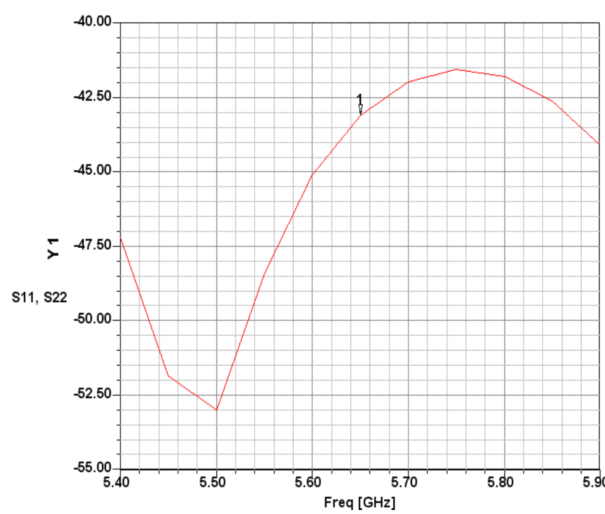

Fig 4(d) Polar plot of S_{11} and S_{22}

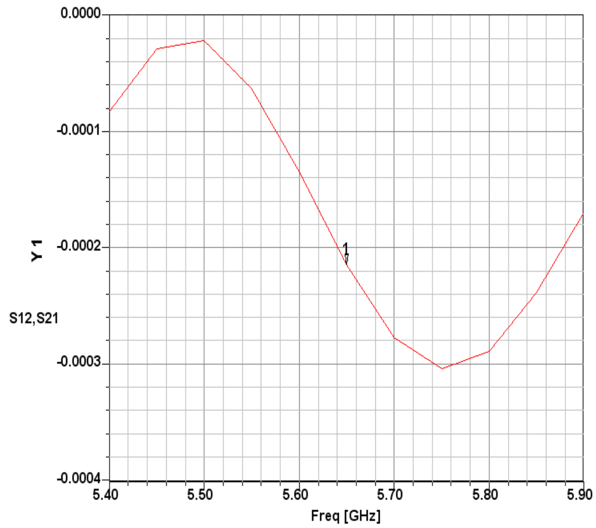

Fig 4(e) Polar plot of S_{12} and S_{21}

D.3 Polarizer was constructed as in Fig 5(a) and assigned perpendicular excitation waveports as in Fig 5(b) and Fig 5(c).

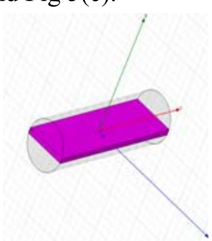
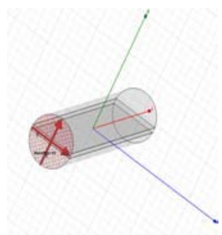
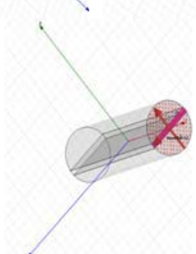

Fig 5(a) Fig 5(b) Fig 5(c)

D.4 Analysis results of Fig 5(a) structure for S_{11},S_{22} ,S_{12} and S_{21} at center frequency of 5.65 GHz are shown in Fig 5(d) and port impedances in Fig 5(e)

Freq		S:WavePort1:1	S:WavePort1:2	S:WavePort2:1	S:WavePort2:2
5.65 (GHz)	WavePort1:1	(0.0068754, 80.1)	(0.00084355, 68.3)	(0.99997, -19)	(0.0018468, -16)
	WavePort1:2	(0.00084355, 68.3)	(0.044326, 168)	(0.0018805, -116)	(0.99901, 67.3)
	WavePort2:1	(0.99997, -19)	(0.0018805, -116)	(0.0068757, 61.9)	(0.00076297, 161)
	WavePort2:2	(0.0018468, -16)	(0.99901, 67.3)	(0.00076297, 161)	(0.044329, 147)

Fig 5(d) Analysis result of S_{11},S_{22} ,S_{12} and S_{21}

Freq		Port Zo
5.65 (GHz)	WavePort1:1	(117.84, 2.67e-005)
	WavePort1:2	(131.74, 0)
	WavePort2:1	(118.6, 0)
	WavePort2:2	(132.9, 0)

Fig 5(e) port impedances

D.5 Polarizer was added to the ferrite rod as shown in Fig 6(a) and uniform magnetic bias of 240000A/m (transverse) was assigned as in Fig 6(b) and waveports were assigned as in Fig 6(c) and Fig 6(d)

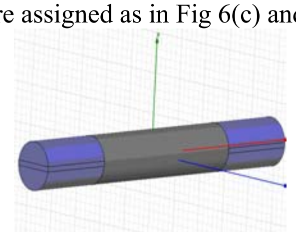
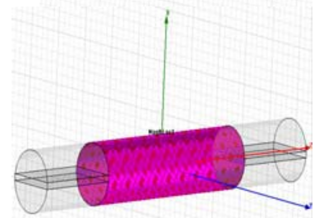

Fig 6(a) Fig 6(b)

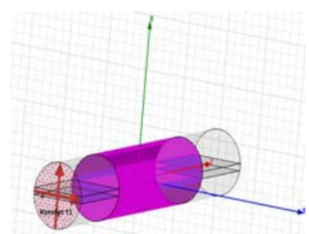
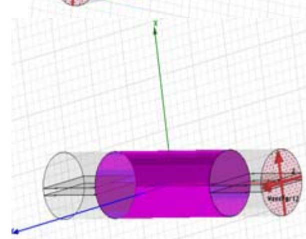

FIG 6(C) FIG 6(D)

D.6 Analysis results for Fig 6(a) structure for S_{11},S_{22} ,S_{12} and S_{21} is shown in Fig 6(e) and Fig 6(f) over frequency sweep from 5.4 GHz to 5.9 GHz

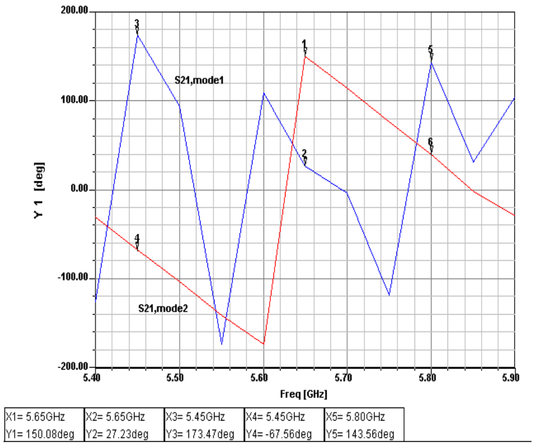

Fig 6(e) Analysis results for Fig 6(a) structure for S_{21}

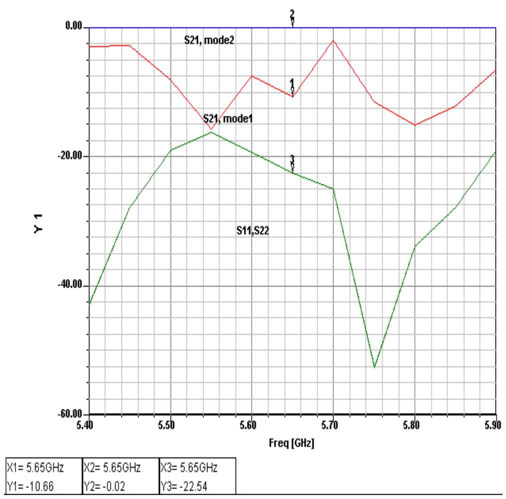

Fig 6(f) Analysis results for Fig 6(a) structure for S_{11},S_{22} ,S_{12} and S_{21}

D.7 Similarly, uniform magnetic bias of 240000A/m (longitudinal) and waveports were assigned to Fig 6(a) structure .Analysis results for S_{11},S_{22} ,S_{12} and S_{21} is shown in Fig 6(g) and Fig 6(h) over frequency sweep from 5.4 GHz to 5.9 GHz and Fig 6(i) shows the phase shift which is -185.49 degrees.

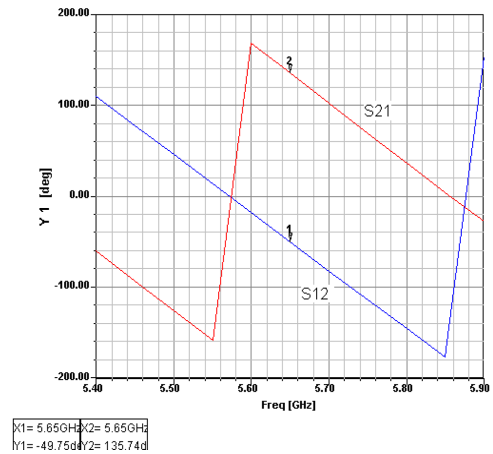

Fig 6(g) Analysis results for Fig 6(a) structure for S_{12} and S_{21} with magnetic bias

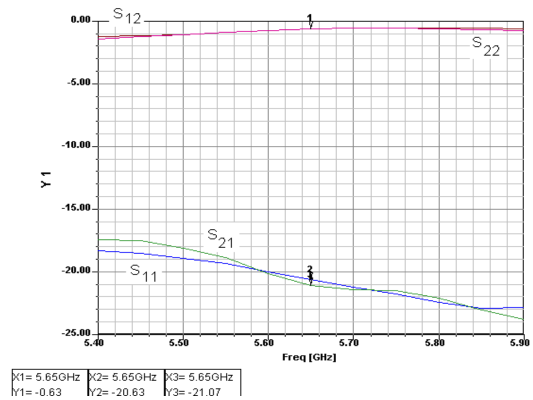

Fig 6(h) Analysis results for S11,S22 ,S12 and S21 for Fig 6(a) structure with magnetic bias

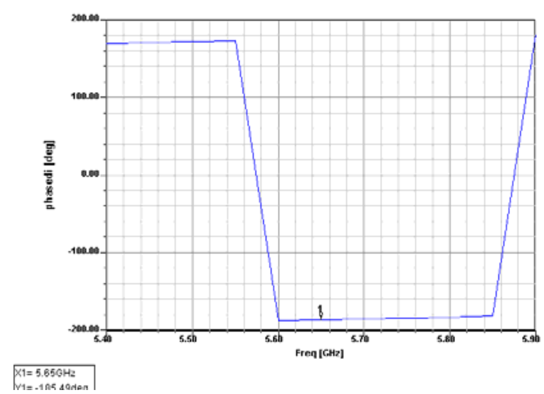

Fig 6(i) Phase shift -185.49 degrees for Fig 6(a) structure

D.8 Brass housing was added on either sides as in Fig 7(a), matching section was subtracted from it as in Fig 7(b).

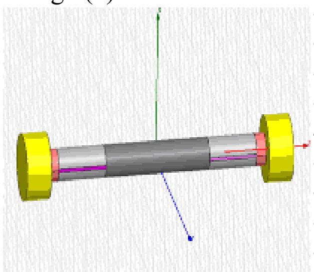

Fig 7(a)

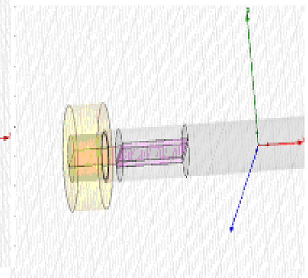

Fig 7(b)

D.9 Fig 7(c) shows analysis results for S_{11},S_{22} and Fig 7(d) shows analysis results S_{12} and S_{21} after assigning waveports to Fig 7(a)structure.

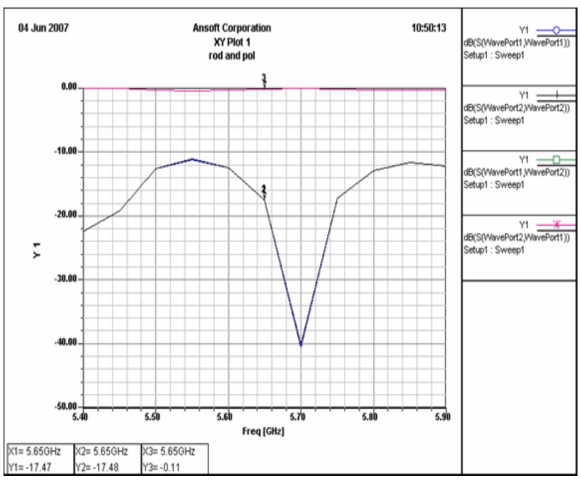

Fig 7(c) Analysis results for S_{11},S_{22} for 7(a) structure

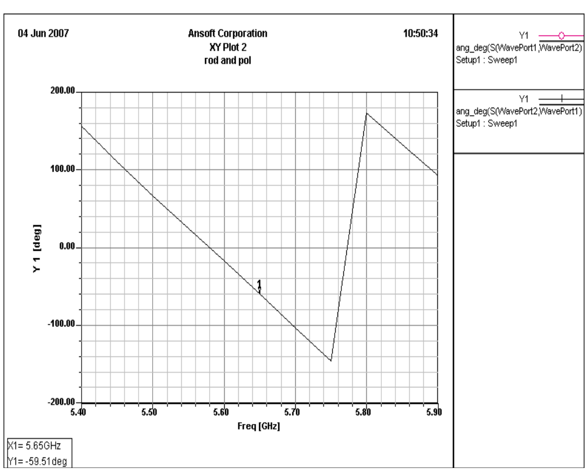

Fig 7(d) Analysis results for S_{12} and S_{21} for 7(a) structure

II. RESULT

Structure in Fig 8(a) is similar to the one drawn for the matching section analysis with rotated polarizers by 45 degrees, so as to convert a linearly polarized wave to circularly polarized wave at the output of the input end polarizer and vice-versa is true for output end polarizer .Thereby, completing the design of Ferrite rotary vane phase shifter.

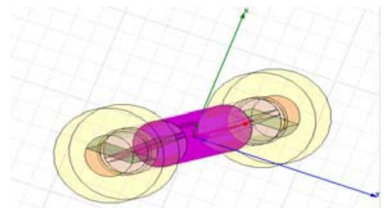

Fig 8(a) Rotary vane ferrite phase shifter

By magnetising ferrite rod in transverse direction we get plots as in Fig 8(b) and 8(c), thereby giving phase shift (transverse magnetize) as 118.26 degrees

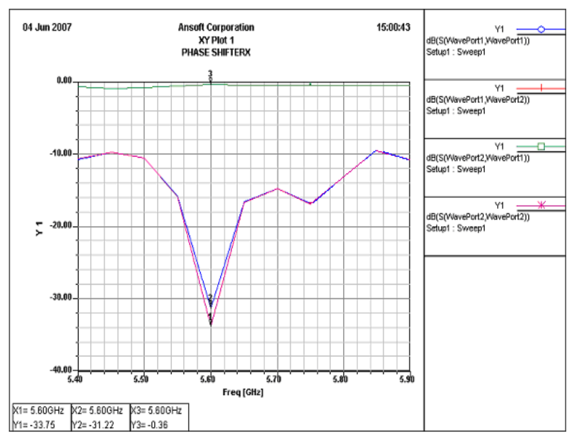

Fig 8(b) Phase plot of S_{11},S_{22} ,S_{12} and S_{21}

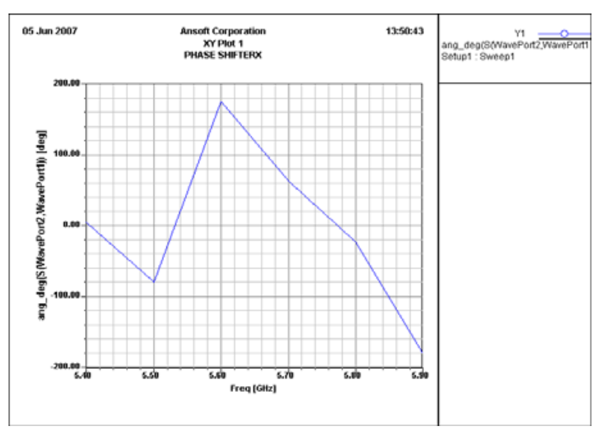

Fig 8(c) Phase plot of S_{21}

Next by magnetising ferrite rod in longitudinal direction we get plots as in Fig 9(a) and 9(b), thereby giving phase shift (longitudinally magnetize) as -54.6 degrees.

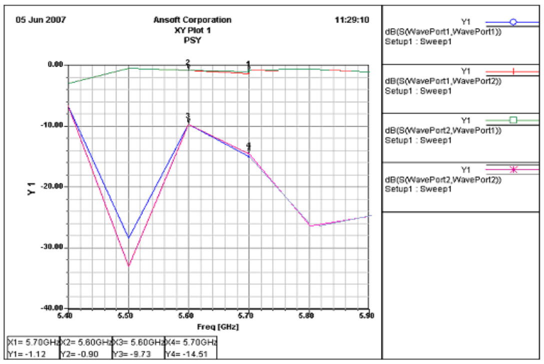

Fig 9(a) Phase plot of S_{11}, S_{22} , S_{12} and S_{21}

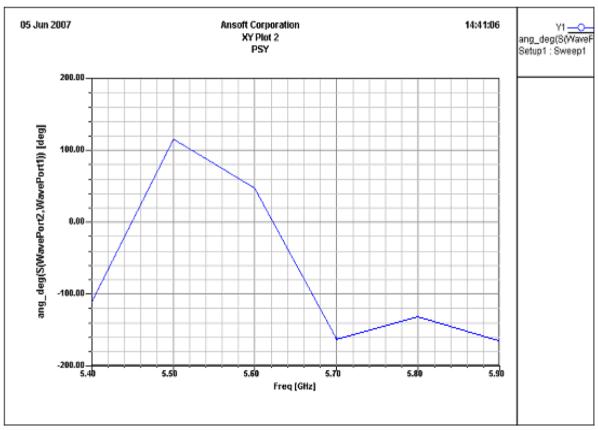

Fig 9(b) Phase plot of S_{21}

THUS, TOTAL PHASE SHIFT = 118.26- (-54.6)

$$= 172.86^{\circ} \quad (\approx 180^{\circ})$$

It has been proved that by giving a phase shift of 90 degrees to the magnetic field, we will get the phase shift of twice the rotation i.e. 180 degrees.

REFERENCES

[1] K.Kupfer, A.Kraszewski, and R.knochel. RF and microwave sensing of moist materials, food, and other dielectrics.Sensors Update, Jan.2000, Vol.7.

[2] S.Trabelsi and S.O.Nelson, and P.G.Bartley Jr. Coaxialdielectric sensor for cereal grains. IEEE Instrum.Meas.Technolgy. May 20-22,2003.

[3] Samir Trabelsi, Andrzej W Kraszewski and Stuart O Nelson. Nondestructive microwave characterization for determining the bulk density and moisture content of shelled corn.Meas.Sci.Technol.1998.

[4] Gao Jianping, Zhang Zhixian. Electric wave transmission, Xi'an: Northwestern technical university publication, 2002.

[5] Xu Longxiang. The iterative computation new method of optimum Pyramid horn antenna. control guidance and fuze ,1996,1:44-46